American Mineralogist, Volume 73, pages 1025–1037, 1988

Pyroxenes and fayalites in the Bandelier Tuff, New Mexico: Temperatures and comparison with other rhyolites

CHARLOTTE M. WARSHAW,* ROBERT L. SMITH**
U.S. Geological Survey, Reston, Virginia 22092, U.S.A.

ABSTRACT

Ferromagnesian silicates and magnetite are found throughout the Pleistocene Bandelier Tuff, Jemez Mountains, New Mexico. The upper (Tshirege) member of this rhyolitic ash-flow formation repeats the general type of sequence found in the lower (Otowi) member, a basal pumice air-fall unit followed by a succession of many ash flows. Clinopyroxene coexists with fayalite in the basal air fall and succeeding ash flows of each member and with orthopyroxene in its later flows. The compositions of these minerals range from Fe-rich at the base of each member to less Fe-rich at its top. This gradual change is related to the variation in chemical composition and temperature of the magma in the zoned magma chamber for each eruptive cycle. The ferrohedenbergite ($Ca_{43}Mg_8Fe_{49}$) and fayalite ($Fe_{87.3}Mn_{8.8}Mg_{3.5}Ca_{0.4}$) of the basal air fall of the Tshirege Member formed at the lowest temperature (~700 °C). The uppermost, or last erupted, ash flow has the most Mg-rich augite ($Ca_{41}Mg_{37}Fe_{22}$) and hypersthene ($Ca_3Mg_{52}Fe_{45}$) and had a pre-eruptive temperature close to 850 °C. The regularity of the variation in composition and temperature throughout the Tshirege Member exists, undoubtedly, because all these phases crystallized from magma in the same zoned chamber.

The types and compositions of the ferromagnesian silicates of the Bandelier Tuff are related to the oxygen fugacity. A comparison of the chemical composition of the Bandelier Tuff samples and other rhyolites described in the literature indicated that, in general, higher oxygen fugacities could be related to lower agpaitic indices and lower Fe/Ca ratios. The Bandelier Tuff and certain other rhyolites on or below the FMQ oxygen-buffer curve have subaluminous compositions and higher Fe/Ca molar ratios (>1.9) than those of high-silica rhyolites located on higher oxygen buffer curves.

INTRODUCTION

The occurrence of pyroxenes and fayalites in the Bandelier Tuff was reported by Smith and Bailey (1966). The chemical composition and mineralogical properties of these phases and the correlation of the former with the stratigraphy of the tuff and with the pre-eruptive temperature and oxygen fugacity of the magma are the principal concerns of the present paper. A secondary concern is the determination of relationships between the types and compositions of the ferromagnesian silicate phenocrysts and the whole-rock compositions within the Bandelier Tuff and in similar rhyolites described in the literature.

The Bandelier Tuff

The Bandelier Tuff, a Pleistocene rhyolite formation in the Jemez Mountains, New Mexico, has been described in preliminary papers by Smith and Bailey (1966), Bailey et al. (1969), and Smith (1979). The formation was subdivided into upper (Tshirege, 1.1 Ma) and lower (Otowi, 1.45 Ma) members, each consisting of a basal air fall overlain by a succession of ash flows showing varying degrees of welding. The formation, which has an outcrop area of about 1300 km², is exposed in canyons that dissect plateaus flanking the Valles Caldera, the center of which is about 25 km west of Los Alamos. Smith and Bailey (1966) presented evidence that each member is the product of a single caldera-forming eruption with numerous pulses from a magma chamber that was zoned chemically and thermally. The upper member erupted after an interval of about 350 000 yr, during all or part of which time the thermal and chemical zonation, similar to that of the lower member, was recovered.

Smith and Bailey (1966) mentioned that the upper and lower members of the Bandelier Tuff are similar in physical and chemical properties and gave details of these properties for only the upper (Tshirege) member in their preliminary study. They subdivided the Tshirege Member into five subunits on the basis of mineralogy and thermal characteristics as shown by degrees of welding or of devitrification (Smith and Bailey, 1966, Figs. 8–12, p. 8–14). In the present paper, subunit I consists solely of the Tsankawi Pumice Bed, the basal air fall, as shown in Table 1. Smith and Bailey (1966) found that the abun-

* Present address: 3703 Stewart Driveway, Chevy Chase, Maryland 20815, U.S.A.
** Present address: U.S. Geological Survey, 2943-C Fulton Avenue, Sacramento, California 95821, U.S.A.

0003–004X/88/0910–1025$02.00

TABLE 1. Description of samples listed in sequence from top of Tshirege Member, Bandelier Tuff, to its basal air fall

Subunit*	Sample number	Ferromagnesian silicates**	Dominant feldspar	Locality, 15′ quadrangle
V or Anorthoclase Unit	6	cpx, opx	anorthoclase	Frijoles
IV	7	cpx, opx	anorthoclase	Frijoles
	5	cpx, opx	anorthoclase, sanidine	San Ysidro
III	B2	cpx, opx, fa	sanidine	San Ysidro
	2	cpx, opx, fa	sanidine	Abiquiu
	3	cpx, fa	sanidine	Abiquiu
II	B8	cpx, fa	sanidine	Abiquiu
	30	cpx, fa	sanidine	Abiquiu
	B9	cpx, fa	sanidine	Abiquiu
	B4	cpx, fa	sanidine	Jemez
	1	cpx, fa	sanidine	Espanola
I or Tsankawi Pumice Bed	B5	cpx, fa	sanidine	Espanola

Note: The prefix "B" for Bandelier on some of the sample numbers was used in an earlier numbering system.

* This composite section does not indicate thickness or volume of the subunits.

** Abbreviations: cpx, clinopyroxene; opx, orthopyroxene; fa, fayalite.

dance of phenocrysts increases from subunit I, which came from the top of the magma chamber, through subunit V, the last erupted ash flows of the Tshirege sequence. In addition to the phenocrysts shown in Table 1, quartz is also present in all but subunit V. The Tshirege Member contains microphenocrysts of magnetite and ilmenite, and traces of zircon, apatite, chevkinite, and allanite. Not all of these occur in every subunit.

In their preliminary chemical studies, Smith and Bailey (1966) found that the Bandelier Tuff is composed essentially of high-silica (76–77%) rhyolite except for subunit V, which has 72% SiO_2. The CIPW norm for an unpublished analysis of one of the Bandelier Tuff samples suggested that 97 wt% of the anhydrous portion of the magma might consist of silica and aluminosilicate networks. Mahood and Hildreth (1983) stated that 98 mol% of certain high-silica rhyolites consists of silica, alumina, and alkalies and alkaline earths for charge-balancing. Seifert et al. (1982) using Raman spectra determined the different three-dimensional structural configurations in such silicate melts. All the oxygens in these structures are the bridging type, i.e., there are no nonbridging oxygens per tetrahedral ion (NBO/T = 0).

Evidence for the chemical gradient within the magma chamber was obtained by Smith and Bailey (1966) by plotting the amounts of Fe, Mg, alkalies, halogens, and some trace elements in samples of the tuff against the stratigraphic sequence from subunits I through V. This early preliminary study revealed changes in the types of ferromagnesian silicates but gave no data on the chemical composition of these phases.

The initial results of the present study were reported by Warshaw and Smith (1980), with the conclusion that the compositions of the ferromagnesian silicate phenocrysts in the Bandelier Tuff differed significantly from those occurring in a couple of other high-silica rhyolites, e.g., the Bishop Tuff (Hildreth, 1977).

Other studies

Earlier studies of ferromagnesian silicates in low-magnesia, high-silica rhyolites were made by Hildreth (1977, 1979) and Mahood (1980, 1981). The Bandelier Tuff clinopyroxenes had the widest range for a silicic volcanic suite from a single eruption for which Warshaw and Smith (1980) had yet seen pyroxene analyses. Hildreth (1981) reported that the clinopyroxenes of the eruptive sequence associated with the formation of the Yellowstone Caldera have the same compositional range as those of the Bandelier Tuff. Hildreth et al. (1984) showed that this range was for both the Lava Creek Tuff and the Upper Basin Member of the Plateau Rhyolite, the latter being postresurgence moat rhyolites from the same magma chamber as the Lava Creek Tuff.

Carmichael (1967) found that the wide range in the relative amounts of Fe and Mg in the pyroxenes from many different salic volcanic rocks was not related to temperature. It was influenced by the prior crystallization of Fe-Ti oxides, by magnetite more than by ilmenite. The "iron ratios," 100(Fe + Mn)/(Fe + Mn + Mg), of the pyroxenes were lower than those of the whole rocks. However, the same was not true for the fayalites, which were from rocks on a lower oxygen-buffer curve than those that contained orthopyroxenes.

Izett (1981) studied the chemical and physical properties of the glass portion of volcanic rocks. He used the relative amounts of FeO and CaO, as well as the presence of biotite, to separate rhyolitic volcanic ashes into two types. His plot also separated rhyolites from andesites. Izett selected these two oxide components because they showed the largest variation in the analyses. Fayalite phenocrysts were limited to the rhyolite type with high FeO/CaO ratios.

METHODS

Sample selection

The samples in Table 1 were selected, after preliminary laboratory studies of more than a hundred samples, as being representative of different horizons throughout the Tshirege Member of the Bandelier Tuff. Because they are from widely separated sections and because the individual flows vary in thickness between sections, it is not possible to give differences in depth between samples. The sanidine compositions were useful in establishing the sequence, particularly in subunit II. A sample of the Guaje Pumice Bed, the basal air fall of the Otowi Member of the Bandelier Tuff, was also selected for study in order to compare it with the Tsankawi Pumice Bed.

All the minerals of this study were separated from nonwelded pumice lumps consisting of silky, fibrous glass containing 5–30 vol% phenocrysts of feldspar plus quartz. Whenever possible, the minerals of each sample were separated from a single, large, representative pumice lump. Representative grains from the concentrates were mounted and polished for electron-microprobe analyses, while others were examined optically. Some con-

TABLE 2. Optical and crystallographic data for hedenbergite and fayalite from Guaje Pumice Bed

	Hedenbergite	Fayalite
	Refractive indices*	
α	1.727	≤1.814
β	1.733	1.852
γ	1.749	≥1.862
	Cell parameters*	
a	9.810 Å	4.831 Å
b	9.008 Å	10.499 Å
c	5.262 Å	6.103 Å
β	105°35′	
V	447.90 Å³	309.53 Å³

Note: Determined by K. Dickson, U.S. Geological Survey.

centrates were further purified for "wet"-chemical and neutron-activation analyses.

Electron-microprobe analysis

Earlier analyses were made with a manual ARL-EMX electron microprobe. With the automated microprobe used later, the quantitative analysis program of Finger and Hadidiacos (1972) was used together with the Bence-Albee (1968) matrix correction scheme. For all analyses, the operating conditions were 15 kV, 0.1 μA, and 20-s preset time (or 20000 counts). The standards used for the silicate analyses were the same as those used by Huebner and Turnock (1980, p. 249).

With the manual instrument, 4 to 8 points per grain on 5 to 8 grains were probed for each set of three elements, the analysis of each point being repeated. The homogeneity or lack thereof was apparent from the count data. Average elemental compositions were calculated from the raw microprobe data and corrected with program ABFAN (Hadidiacos et al., 1971), which calculates oxide percentages and formulas for pyroxenes based on 6 oxygens.

Most of the earlier analyses were repeated with the automated microprobe, and no significant differences were found between replicates.

Temperature determination

Electron-microprobe analyses were used to calculate the percentages of ulvöspinel (Fe_2TiO_4) in the titanomagnetites and of $FeTiO_3$ in the ilmenites by the Carmichael (1967) method. Fe-Ti oxide geothermometry could be used only on one sample.

Most of the Bandelier ash flows contain magnetite but no ilmenite. The flows containing fayalite (F), magnetite (M), and quartz (Q) should be located on an oxygen-buffer curve displaced from the FMQ buffer for pure fayalite and magnetite. At first, the minimum temperatures of the fayalite-magnetite pairs were estimated by locating them on the Buddington-Lindsley (1964) oxygen fugacity–temperature plot at the intersections of the appropriate magnetite (mt)–ulvöspinel (usp) isopleths with the displaced Hewitt (1978) FMQ buffer curve. The amount of displacement (toward a higher oxygen fugacity) was determined by the method of Simmons et al. (1974). Finally, the minimum temperatures and oxygen fugacities of the samples containing magnetite and fayalite but no ilmenite were determined for a pressure of 2 kbar by D. H. Lindsley (pers. comm.) by the QUIIF (quartz-ulvöspinel-ilmenite-fayalite) method of Frost et al. (1988).

DESCRIPTIONS OF PYROXENES AND FAYALITES

The color of the prismatic clinopyroxene grains ranges continuosly from very dark green in the Tsankawi air fall to light green in subunit V. The latter also contains an olive-green pyroxene, no. 6B. The α' and γ' indices of refraction of cleavage fragments range from 1.730 and 1.751 for the dark-green clinopyroxene (hedenbergite) to 1.699 and 1.719 for the light-green augite.

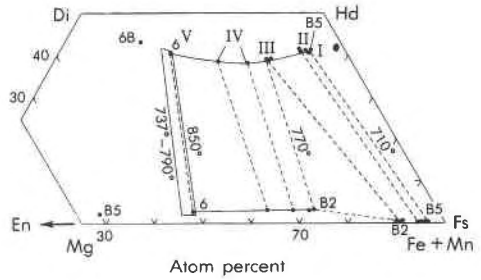

Fig. 1. The compositions of the pyroxene and fayalite phenocrysts from the Tshirege Member of the Bandelier Tuff plotted in terms of Ca, Mg, and Fe + Mn. Roman numerals indicate subunits. Sample numbers are shown for compositional end members. Clinopyroxene no. 6B and orthopyroxene no. B5 are xenocrysts. The apparent equilibrium tie lines, with some calculated temperatures (°C), are dashed. Only one set of tie lines is shown for subunit III. Only two of the tie lines to the fayalites of subunits I and II are drawn. The others of subunit II would be parallel to these. The stippled area between the two solid tie lines enclosing the pyroxenes of subunit V represents the limits of the two-pyroxene field for the Bishop Tuff (Hildreth, 1977). Its temperature range is also shown. The small filled oval indicates the ferrohedenbergite compositions of the rhyolites of the Sierra La Primavera (Mahood, 1980). The corners of the figure are labeled as on the pyroxene quadrilateral: En = enstatite, Fs = ferrosilite, Di = diopside, Hd = hedenbergite.

The optical properties of the hedenbergite from the Tsankawi and Guaje Pumice Beds—Tshirege and Otowi basal air falls, respectively—are the same within the limits of error. Their chemical compositions are also very similar, as will be shown later. Optical and crystallographic data for the dark-green hedenbergite from the Guaje air fall are given in Table 2.

Orthopyroxene in equilibrium with clinopyroxene is not found below the top of subunit III in the Tshirege Member and is rare in the earliest flows in which it first appears. The color observed with a binocular microscope ranges from light brown in the lower samples to light tan in the uppermost ash flows, as the highest refractive index of the cleavage fragments decreases from 1.745 to 1.720. The pleochroic colors are pinkish tan and pale green.

The fayalites are smooth, glossy, honey-colored spheroidal grains ranging from 0.5 mm to more than 1.0 mm. The larger grains show some development of crystal faces but still have a rounded habit. Optical and crystallographic data for the Guaje fayalite are given in Table 2.

CHEMICAL COMPOSITION

Equilibrium phases

Formulas based on four cations and six oxygens for the pyroxenes and on three cations for the fayalites were derived from the average chemical compositions deter-

TABLE 3. Average chemical analyses and formulas of clinopyroxenes in Bandelier Tuff

Member:	Air falls			Ash flows		
	Otowi		Tshirege	Tshirege		
Pumice bed:	Guaje	Guaje	Tsankawi			
Subunit:			I	bottom II	top III	top V
Sample number:			B5	1	B2	6
Chemical method:	"wet"*	electron microprobe				
	Weight percent**					
SiO_2	48.5	48.27	48.67	48.48	49.34	51.48
Al_2O_3	0.3	0.29	0.29	0.30	0.28	0.91
Fe_2O_3	2.6					
FeO	24.8	27.22	26.84	26.97	23.44	13.02
TiO_2	0.13	0.08	0.08	0.08	0.10	0.21
MgO	2.4	2.28	2.36	2.46	5.61	12.36
MnO	2.9	2.80	2.53	2.57	1.96	1.10
CaO	18.2	18.26	18.23	18.16	17.87	19.06
Na_2O	0.7	0.62	0.65	0.59	0.48	0.53
Total	100.2	99.82	99.65	99.61	99.08	98.67
	Formulas					
	Basis of 6 oxygens	Basis of 4 cations and 6 oxygens				
T Si	1.972	1.971	1.987	1.981	1.985	1.972
T Al	0.014	0.014	0.014	0.014	0.013	0.028
M Al						0.013
M Fe^{3+}	0.080	0.089	0.059	0.065	0.049	0.041
M Fe^{2+}	0.843	0.841	0.858	0.856	0.740	0.376
M Ti	0.004	0.002	0.002	0.002	0.003	0.006
M Mg	0.145	0.139	0.144	0.150	0.336	0.706
M Mn	0.100	0.097	0.087	0.089	0.067	0.036
M Ca	0.793	0.799	0.797	0.795	0.770	0.782
M Na	0.055	0.049	0.051	0.047	0.037	0.039
Total T	1.986	1.985	2.001	1.995	1.998	2.000
Total M	2.020	2.016	1.998	2.004	2.002	1.999
Total wt% with Fe_2O_3	100.2	100.11	99.84	99.82	99.24	98.81

* J. Marinenko, U.S. Geological Survey

** Wt% Zn by neutron-activation analysis (P. Baedecker, U.S. Geological Survey): no. B5, 0.085; no. 1, 0.082; no. 5 (subunit IV), 0.06; no. 6, 0.04.

mined by electron-microprobe analysis. This necessitated converting some of the FeO in the microprobe analyses of the pyroxenes to Fe_2O_3 to maintain charge balance. Percentages of Wo, En, and Fs were calculated from the atomic proportions of Ca, Mg, and total Fe plus Mn, and these percentages were plotted on the pyroxene quadrilateral in Figure 1. Fayalites are shown near the ferrosilite corner. The progressive variation in composition from right to left along the trends shown for each phase on the diagram is in accordance with the stratigraphic sequence shown in Table 1; therefore, sample numbers are not shown for all the plotted points.

Complete analyses for the clinopyroxenes from the air falls and from the lowest and highest ash flows of the Tshirege Member of the Bandelier Tuff are given in Table 3. Also shown is the analysis of an augite from subunit III that was found associated with both fayalite and hypersthene. The compositions of the fayalites and hypersthenes found together with the clinopyroxenes of Table 3 are given in Table 4. The percentage of MnO was found to be highest in the Guaje fayalite and is the highest we have ever seen reported for a magmatic fayalite.

The "wet"-chemical analyses of a few of these samples agree very well with the microprobe analyses given in Tables 3 and 4, including the percentages of Fe_2O_3 found by calculating these stoichiometric formulas. One example, the Guaje clinopyroxene, is shown in Table 3. The percentages of FeO and Fe_2O_3 found by calculation to be 24.6 and 2.9, respectively, should be compared with the values by "wet" chemistry.

As Table 3 shows complete compositions for only five of the pyroxenes plotted in Figure 1, the variation of all the component oxides in 11 of the analyzed Tshirege clinopyroxenes is presented in Figure 2, where formula values are plotted against the amounts of Mg in the formula unit based on four cations. This element increases in the clinopyroxenes from basal unit to uppermost ash flow. Figure 2B shows the minimum in Ca that is observed on the quadrilateral plot at the composition of augite in sample 5, one of the subunit IV samples. It appears that a minimum in Na accompanies the minimum in Ca. Figure 2C indicates that as Mg increases, AL increasingly substitutes for Si in tetrahedral coordination in subunits IV and V.

Heterogeneity and nonequilibrium phases

The clinopyroxenes and fayalites from each of the samples from subunit I through most of subunit III are ho-

TABLE 4. Average chemical analyses and formulas of fayalites and orthopyroxenes in Bandelier Tuff

	Air falls		Ash flows			
Member	Otowi	Tshirege	Tshirege			
Pumice bed	Guaje	Tsankawi				
Subunit		I	bottom II	top III	top III	top V
Sample number		B5	1	B2	B2	6
Phenocryst	Fayalite				Hypersthene	
			Weight percent*			
SiO_2	29.92	30.25	29.70	30.63	48.22	51.52
Al_2O_3	0.00	0.00	0.00	0.00	0.19	0.32
FeO	61.61	61.88	61.78	61.79	38.89	26.96
TiO_2	n.d.	n.d.	n.d.	n.d.	0.14	0.18
MgO	1.28	1.40	1.41	3.77	8.26	17.69
MnO	6.80	6.14	6.30	4.60	2.93	2.06
CaO	0.17	0.19	0.19	0.20	1.52	1.30
Total	99.78	99.86	99.38	100.99	100.15	100.03
			Formulas			
			Basis of 3 cations		Basis of 4 cations and 6 oxygens	
T Si	1.005	1.014	1.001	0.998	1.978	1.980
T Al					0.009	0.014
M Fe^{3+}					0.025	0.015
M Fe^{2+}	1.731	1.735	1.741	1.685	1.309	0.851
M Ti					0.004	0.005
M Mg	0.064	0.070	0.071	0.183	0.505	1.013
M Mn	0.194	0.174	0.180	0.127	0.102	0.067
M Ca	0.006	0.007	0.007	0.007	0.067	0.054
Total T	1.005	1.014	1.001	0.998	1.987	1.994
Total M	1.995	1.986	1.999	2.002	2.012	2.005
No. oxygens	4.005	4.014	4.001	3.998	6.000	6.000
Total wt% with Fe_2O_3					100.23	100.08

* Wt% Zn by neutron-activation analysis (P. Baedecker, U.S. Geological Survey): no. B5, 0.014; no. 5, (subunit IV), 0.09; no. 6, 0.08.

mogeneous. At the top of subunit III, however, the average compositions of some of the clinopyroxene grains of sample B2 vary from the overall average shown in Table 3 by as much as 0.5 and 0.3% FeO and MgO, respectively, with about 10% of the orthopyroxene grains being intermediate between those of samples B2 and 6 in composition (Table 4).

The pyroxenes from subunit IV also show minor intergrain heterogeneity. In additon, some of the orthopyroxene (opx) grains of sample 5 are zoned, with homogeneous cores having a composition slightly more Mg-rich than opx in sample 6, and outer portions becoming increasingly higher in Fe away from the core. These cores may be xenocrysts, as is probably true also for the minor plagioclase found in this sample. The gradual change in the composition of the opx crystals may have occurred at the same time that the overgrowth of sanidine on the anorthoclase was taking place. The outermost portion of these opx grains is considered to be in equilibrium with the bulk of the clinopyroxene.

The orthopyroxene grains obtained from the subunit V sample (no. 6) are homogeneous. Most of the augite from this sample is light green. Its intergrain variation from the average (Table 3) was found to be as large as 1.2 and 0.9% for FeO and MgO, respectively. A minor amount of another clinopyroxene (cpx), designated 6B in Figure 1, is also present. This is olive-green and contains more Mg and less Fe than no. 6, as shown on the quadrilateral plot. The olive-green cpx has twice as much alumina and four times as much titania as the light-green augite. The amounts of these two constituents are even higher, almost 4% alumina and more than 1% titania, in zones that appear to be remnants of a replacement process. This more aluminous pyroxene may have had the same source as the andesine xenocrysts in sample no. 6.

Izett and Wilcox (1968, p. 1561) reported that the Tsankawi Pumice Bed contains hornblende, bronzite, and rare plagioclase in addition to hedenbergite, fayalite, and sanidine. Sample B5, the Tsankawi, was found to have a considerable amount of hornblende and also some orthopyroxene, rare plagioclase, a light-green augite (<0.5% of the total clinopyroxene, the bulk of which is dark-green hedenbergite) and "exsolved" magnetite containing much more magnesia than in the bulk of the magnetite, which is homogeneous. Some crystal clots separated from the heavy-mineral concentrates consist of a combination of all of these minerals. Both the orthopyroxene (opx), plotted in Figure 1, and the light-green augite (cpx) are higher in magnesia (opx, 25.9%; cpx, 14.5%) and alumina (opx, 2.3%; cpx, 1.4%) than any of the Tshirege equilibrium opex and cpx phases and were obviously not formed in equilibrium with the fayalite, hedenbergite, sanidine, and most of the magnetite. The Tshirege Member of the Bandelier Tuff contains some pumice lumps of a rock identified as "hornblende pumice." It is difficult to remove all of these small pumice lumps from samples of the

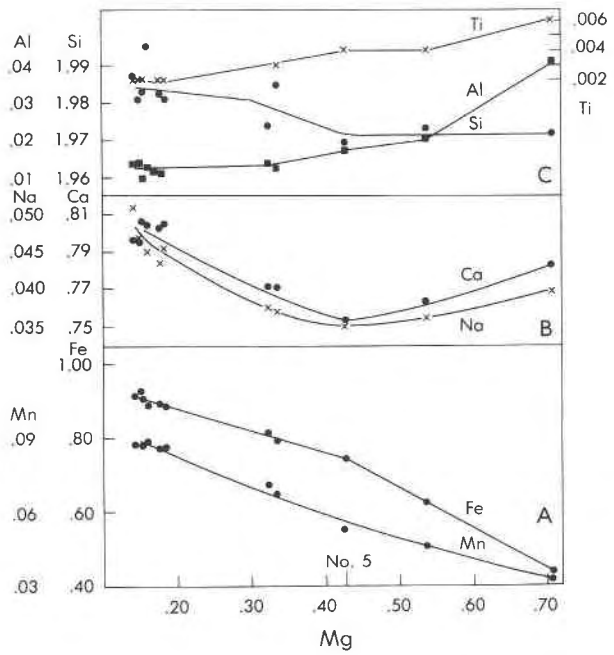

Fig. 2. The amounts of major and minor elements per formula based on 4 cations vs. the amounts of Mg per formula unit for 11 Tshirege clinopyroxenes: (**A**) Fe and Mn; (**B**) Ca and Na; (**C**) Si, Al, and Ti. Sample number is shown at significant change in slope.

TABLE 5. Pre-eruptive temperatures and oxygen fugacities of the Bandelier Tuff determined by different methods

Sub-unit	Sample	Molar fractions* usp	ilm	fay	Oxide-silicate temperature (°C)	$\log_{10} f_{O_2}$	Two-pyroxene temperature** cpx (°C)	opx (°C)
		Part A. Samples containing magnetite but no ilmenite						
	Guaje	0.257		0.8660	696	−16.92		
I	B5	0.260		0.8678	697	−16.90		
II	B4	0.278		0.8690	706	−16.69		
II	1	0.282		0.8701	710	−16.57		
II	30	0.312		0.8610	726	−16.20		
III	B2	0.347		0.8432	746	−15.70	700	800
III	2	0.358		0.8448	753	−15.54		
		Part B. Samples containing magnetite and ilmenite						
IV	5	n.d.	n.d.	no fay			760	800
IV	7	n.d.	0.905	no fay			785	810
V	6	0.364	0.894	no fay	837	−13.01	840	770

Note: In Part A, oxide-silicate values for 2 kbar were determined by D. H. Lindsley (pers. comm.) by the method based on the latest studies of Andersen and Lindsley (1988) and of Frost et al. (1988) on Fe-Ti oxide–silicate equilibria. In Part B, "n.d." signifies "not determined" because the titanomagnetite was not homogeneous and the ilmenite was rare.

* Molar fractions of ulvöspinel and ilmenite were calculated by the Carmichael (1967) method. Molar fractions of fayalite were determined from formulas based on 4 oxygens.

** Values obtained by the method described by Lindsley and Andersen (1983).

Tsankawi air fall; thus, the nonequilibrium phases in sample B5 are probably from the included hornblende pumice, which has the general chemical composition of quartz latite, a dominant rock type of the pre-Bandelier Tschicoma Formation.

Temperature and oxygen fugacity

Minimum temperatures and the corresponding oxygen fugacity for subunits I through III, containing magnetite only, are given in Part A of Table 5.

Oxide temperatures were not estimated for subunit IV because the titanomagnetites are partially oxidized and contain ilmenite lamellae. The temperature and oxygen fugacity for subunit V (Table 5, Part B) were determined by the latest version of the Fe-Ti oxide geothermometer described by Andersen and Lindsley (1988).

The presence of two pyroxenes in the upper ash flows of the Bandelier Tuff suggests that two-pyroxene geothermometers might be used to check the Fe-Ti oxide temperatures. Temperatures obtained with the Lindsley and Andersen (1983) method are given in Table 5.

Figure 3 indicates where the Bandelier Tuff would be located on the oxygen fugacity–temperature plot in the classic paper by Carmichael (1967, Fig. 2). His plot includes several dacites in addition to rhyolites. The Bandelier Tuff samples (●) are plotted according to the earliest determinations (see section on methods) and not according to the later data in Table 5. Figure 3 also includes several high-silica rhyolites, which are more comparable to the Bandelier Tuff. Symbols and references for all the data in Figure 3 are given in Table 6 along with silica percentages and the temperatures as given in the original references. The short solid line below the FMQ buffer curve shows the ranges of temperature and oxygen fugacity of the Lava Creek Tuff according to Hildreth (1981). Dashed lines are shown for some of the other volcanic suites. Bandelier Tuff sample 6 is located on the "pyroxene minus biotite" line. This line is not extended to lower temperatures where biotite may occur just above the FMQ buffer curve (e.g., Hildreth, 1977, 1981). The distance of a plotted point above the FMQ is not only a measure of the oxygen fugacity of a rock but also an indication of the relative values of Fe^{3+}/Fe^{2+} ratios of magmas prior to eruption. The nearly linear relationship between log F_{O_2} and $\log(Fe^{2+}/Fe^{3+})$ at any one particular temperature was determined experimentally by Mysen et al. (1980, 1984), who also gave references to previous studies. It was reported for natural systems by Luhr and Carmichael (1980).

Figure 3 shows higher temperatures and oxygen fugacities for the Bandelier Tuff samples than those in Table 5, Part A, mostly because of the use of the Hewitt (1978) FMQ data rather than the Haas FMQ data used by Frost et al. (1988).

Discussion

Correlation of pyroxene composition with stratigraphy

The compositions of the Tshirege Ca-rich pyroxenes extend from near the hedenbergite side of the pyroxene

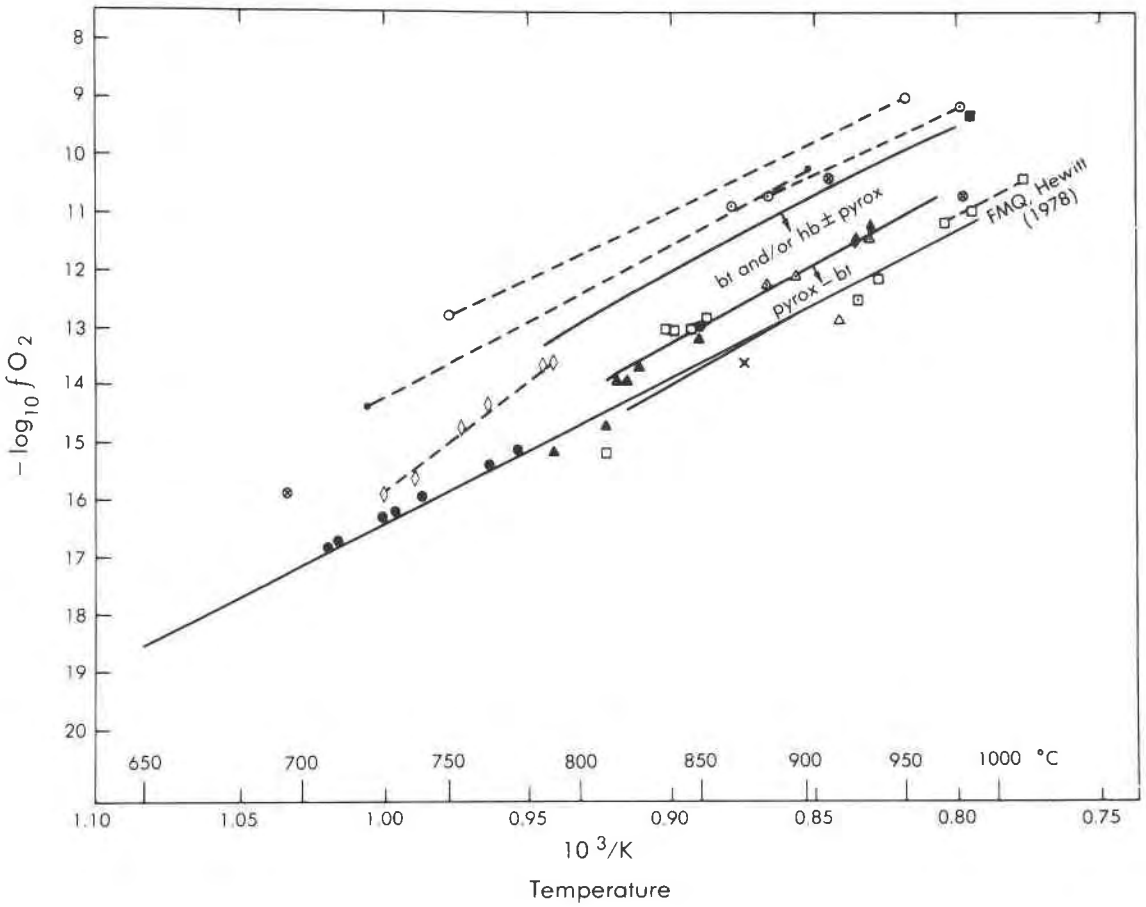

Fig. 3. Plot of oxygen fugacity vs. $1/T$ (10^3/K) for salic volcanic rocks. Their symbols, characteristics, and literature references are listed in Table 6. Celsius temperatures are shown for easy reference to the literature. The line close to, but slightly below, the FMQ indicates the range of the Lava Creek Tuff.

quadrilateral (Fig. 1) for subunit I, the basal air fall, to compositions with more than 50% diopside for subunit V, the uppermost ash flow. The Lava Creek Tuff (Hildreth et al., 1984) is similar to subunits I through III of the Tshirege Member of the Bandelier Tuff, as its clinopyroxenes (cpx) are in equilibrium with fayalite (Fa_{90-96}) and cover the same range of composition except that the youngest Lava Creek Tuff cpx is slightly more to the diopside side of the pyroxene quadrilateral than is the top of subunit III. The oldest part of the Upper Basin Member, which overlies the Lava Creek Tuff, may be similar to subunit IV with respect to clinopyroxene composition and the occurrence of low-Ca pyroxene instead of fayalite.

The correlation of the variation in composition of the pyroxenes (Figs. 1, 2 and Tables 3, 4) and of the preeruptive temperature (Table 5) with the stratigraphic sequence (Table 1) gives evidence for the zonation of the magma chamber in addition to that given by Smith and Bailey (1966). The chemical and mineralogical zoning evident for the Bandelier and some other silicic magma chambers is not explained by any simple process of fractional crystallization. Shaw et al. (1976) and Smith (1979) attributed it to "thermogravitational diffusion" aided by convection in the silicate liquid. Hildreth (1981) described this process in detail in relation to his research on the Bishop Tuff (Hildreth, 1976, 1977, 1979) and gave numerous references to other research on rocks from zoned silicic magma chambers.

Geobarometry

The two orthopyroxenes from the top of subunit III are the most Fe-rich. They coexist with the most Mg-rich fayalites, which indicates that there is a four-phase region (cpx, opx, fa, qtz) in which the compositions of these silicate phases are close to those shown in Figure 1 for subunit III. The appearance of the quadrilateral based on the proportions of Ca, Mg, and total Fe is almost identical with that in Figure 1, which includes Mn with the Fe. The maximum Fe/(Ca + Mg + Fe) for orthopyroxene, sample B2 of subunit III, is 0.70. The oxide temperature (shown in Fig. 1 as 770 °C) and the compositions of the B2 orthopyroxene and fayalite indicate that the pressure must have been between 1.5 and 2 kbar according to D. H. Lindsley (pers. comm.). A pressure of somewhat less than 2 kbar indicates a shallow depth for a significant portion of the Bandelier magma chamber.

TABLE 6. Symbols, references, and characteristics for volcanics plotted in Figs. 3 and 4

Sample identification and/or locality*	Rock type*	SiO_2** (%)	Total Fe as FeO** (%)	Ferromagnesian phenocrysts	T (°C)
		×: Sierra La Primavera, Mexico (Mahood, 1980)			
South-central dome	rhyolite	76.85	1.77	ferrohd, fa	870†
		◆: Lava Creek Tuff, Wyoming (Hildreth, 1981)			
Early	rhyolite	~77	1.1	hd, fa	820
Late	rhyolite	~75.5	1.8	aug, fa	900
		●: Bandelier Tuff			
Guaje Pumice Bed	rhyolite	76.83	1.32	hd, fa	696
Tsankawi Pumice Bed					
I, B5	rhyolite	76.47	1.59	hd, fa	697
II, 1	rhyolite	76.37	1.50	hd, fa	710
II, 30	rhyolite	76.28	1.47	hd, fa	726
III, 2	rhyolite	76.74	1.38	aug, hy, fa	753
V, 6	rhyolite	72.11	1.96	aug, hy	837
		▲: Mono Craters, California (Carmichael, 1967)			
6	rhyolite	76.69	1.03	fa, hb	790
5	rhyolite	76.73	1.03	fa, hb	810
19	rhy.-obs.	76.71	1.03	trace opx	815
16	rhy.-pum.	76.53	1.02	trace opx	820
17	rhy.-obs.	76.69	1.02	trace opx	825
15	rhy.-obs.	76.70	1.02	trace opx	850
		◇: Bishop Tuff, California (Hildreth, 1977)			
104	rhyolite	77.5	0.79	bt	725
88	rhyolite	77.4	0.67	bt, aug, hy	737
107	rhyolite	76.5	0.85	bt, aug, hy	756
72	rhyolite	75.5	1.06	bt, aug, hy	763
78	rhyolite	75.5	1.07	bt, aug, hy	785
77	rhyolite	75.9	1.01	bt, aug, hy	790
		⊗: Kern Plateau, California (Bacon and Duffield, 1981)			
Long Canyon	rhyolite	76.9	0.46	bt	695
Little Templeton	rhyolite	74.1	1.65	bt	
Templeton	rhyolite	74.0	1.62	bt, hb, hy	910
Monache	rhyolite	72.8	1.96	bt, fa, grt	950
		●: Paintbrush Tuff, Nevada (Lipman, 1971; Lipman et al., 1966)			
Topopah Spring Member	rhyolite	77.4	0.89	bt	720
Topopah Spring Member	qtz. lat.	68.8	2.0	bt, cpx, hb	900
		○: Los Chocoyos Ash, Guatemala (Rose et al., 1979)			
High-K	rhyolite	77.4	0.78	bt	750
Low-K	rhyolite	75.7	1.53	hb, cum	950
		□: Volcán Ceboruco, Mexico (Nelson, 1979)			
104	rhyolite	74.10	1.42	aug, opx	810
122	rhy.-dac.	70.38	2.17	bt	855
364	rhy.-pum.	70.47	2.15	hb	845
346	rhy.-pum.	69.45	2.41	hb	838
348	rhy.-pum.	69.65	2.39	hb	835
136	andesite	56.63	7.80	aug, opx, fo	935
30	andesite	61.55	5.60	aug, opx	987
117	andesite	61.30	5.68	aug, opx	970
61	andesite	59.84	6.25	aug, opx	1015
		△: Glass Mountain, Medicine Lake, California (Carmichael, 1967)			
12	rhy.-obs.	73.85	1.67	pyrox	880
14	rhy.-obs.	73.67	1.69	pyrox	930
13	rhy.-dac.	68.54	3.06	pyrox	895
		△: Iceland (Carmichael, 1967)			
Oraefajokull	obsidian	71.98	3.41	ferrohd, fa	915
Thingmuli	obsidian	72.6	3.12	fa	925
		◆: Inyo Craters, California (Carmichael, 1967)			
23	rhy.-obs.	71.74	1.95	bt, hb	920
24	rhy.-obs.	70.47	2.20	bt, hb	930
		⊙: Lassen, California (Carmichael, 1967)			
28	dacite	71.58	2.53	hb, bt	865
29	dacite	70.15	2.53	hb, bt	880
27	dacite	70.16	2.46	hb, bt	980
		■: Volcán Colima, Mexico (Luhr and Carmichael, 1980)			
9	andesite	61.20	5.07	hb, aug, opx	986

Note: Abbreviations: rhy.-obs., rhyolitic obsidian; rhy.-pum., rhyolitic pumice; qtz. lat., quartz latite; rhy.-dac., rhyodacite; ferrohd, ferrohedenbergite; fa, fayalite; hd, hedenbergite; aug, augite; hy, hypersthene; hb, hornblende; opx, orthopyroxene; bt, biotite; grt, garnet; cpx, clinopyroxene; cum, cummingtonite; fo, forsterite; pyrox, pyroxene.

* Sample designations and rock types are those used in the original references.

** H_2O (and halogen)–free, normalized to 100.0%.

† Rounded low by Warshaw.

The four-phase triangle in the pyroxene quadrilateral, which is based solely on the proportions of Ca, Mg, and total Fe, is almost identical in location (composition of cpx, opx, fa) to that for 800 °C and 1–2 kbar in Figure 6 of Lindsley (1983, p.482).

Relationships among composition, temperature, and oxygen fugacity

Temperature and pyroxene composition. As shown in Figure 1, the pre-eruptive temperature of the Tshirege Member of the Bandelier Tuff increases with increasing Mg content of the pyroxenes and fayalites. The same relationship between temperature and composition of the ferromagnesian silicates exists for the Lava Creek Tuff (Hildreth et al., 1984). The composition ranges of these phases are the same for both tuffs, but temperatures determined for the Lava Creek Tuff are much higher, 820 °C to 900 °C vs. 710 °C to about 770 °C for subunits I through III of the Tshirege Member. The compositions of two other high-silica rhyolites are shown in Figure 1. The clinopyroxenes of the Sierra La Primavera of Mexico (Mahood, 1980, 1981) have a much higher Fe content than the lowest-temperature Bandelier Tuff sample, but the La Primavera volcanics are in the same temperature range as the Lava Creek Tuff. Some of the Bishop Tuff pyroxenes (Hildreth, 1977) are more Mg-rich than those of sample no. 6, but all the Bishop samples have lower temperatures (737 °C to 790 °C) than no. 6. Thus a correlation between temperature and increasing proximity to the diopside side of the pyroxene quadrilateral is possible only for one particular eruption from a single zoned magma chamber. The pyroxene and fayalite compositions must be primarily a function of the oxygen fugacity and composition of the magma including volatiles (Hildreth, 1981) and may be more closely related to the chemical gradient than to the thermal gradient, though related to both. The relationship between pyroxene composition and temperature is clearly illustrated by Lindsley and Andersen (1983).

Whole-rock composition. The Bandelier Tuff and other high-silica rhyolites vary greatly in the types and compositions of the ferromagnesian silicate phenocrysts they contain. These differences are related to the oxygen fugacities of the magmas, as was shown by Carmichael (1967) and is indicated in Figure 3. Therefore, it is of interest to consider some of the compositional differences within the Bandelier Tuff and in other rhyolites that might be related to phenocryst type and oxygen fugacity. Mg, Fe, and the Al and Ca in excess of that included in the three-dimensional framework would be the elements most likely to be related to the oxygen fugacity of the magma because their silicates would have NBO/T > 0. Smith and Bailey (1966) found the percentages of total iron oxides in the Bandelier Tuff to be much higher than those of magnesia. Magnesia is very low (as low as 0.01% according to Hildreth, 1981) in all the high-silica rhyolites, the pyroxenes of which are plotted in Figure 1. Therefore, Fe and Ca were considered the elements most likely to be related to the oxygen fugacity of different rhyolitic magmas. Ca is more basic than either Fe or Mg; therefore, relatively more Ca might be associated with higher oxygen fugacity. In fact, Douglas et al. (1965) stated that previously reported experimental evidence had always shown that the proportion of a redox ion in the higher oxidation state increased with the basicity of a glass or melt.

Figure 4 is a plot of total FeO vs. CaO. Smith and Bailey (1966) gave some data on the FeO content of the Bandelier Tuff but no information on the CaO content. Previously unpublished data on the latter have been used in Figure 4. Values for more than rhyolites are plotted in order to compare the results with those of Izett (1981). The references and symbols for the points in Figure 4 are the same as those in Figure 3 and are given in Table 6 along with the percentages of FeO and SiO_2 and types of rocks and ferromagnesian phenocrysts. All of these features are delineated in Figure 4. A dot-dash line is sketched to show which rocks may be considered to be Fe-rich relative to the amounts of CaO and silica. In a comparison of Figures 3 and 4, it appears that, when Fe is high relative to CaO and silica, a smaller proportion of Fe is in the 3+ state before eruption.

Relationship between oxygen fugacity and magma composition. A progression from fayalite through orthopyroxene to hornblende is shown in both Figures 3 and 4. This progression suggests a possible relationship among oxygen fugacity, Fe^{3+}/Fe^{2+} ratio, and FeO/CaO. The indicated relationships agree with the results of the Raman and Mössbauer spectroscopic studies of Mysen et al. (1979, 1980, 1984). They showed that changes in the melt structure and increases in the Fe^{3+}/Fe^{2+} ratio were related in part to decreasing amounts of Fe relative to alkaline earths or to an increase in the CaO/(CaO + MgO) ratio. In high-silica rhyolites that contain very little magnesia, larger amounts of CaO are comparable to higher CaO/(CaO + MgO) ratios.

The relationships shown in both Figures 3 and 4 are summarized in Table 7 together with some other whole-rock data for rhyolites containing 75% to 77% SiO_2, which includes most of the Tshirege Member of the Bandelier Tuff. Temperatures are given in Table 6. Table 7 shows that oxygen fugacity generally increases with decreasing FeO/CaO and Al-saturation indices. Spaces separate the rocks into groups based on significant differences in these ratios. Similar tables could be prepared for the other silica ranges, but only the one that includes Bandelier Tuff sample 6 is also included in Table 7. Not all of the Tshirege Member samples listed in Table 1 are listed here, because of the lack of temperature or whole-rock compositional data.

The relation between oxygen fugacity and rock type, e.g., slightly peralkaline, subaluminous, alkali-calcic, was stressed when a condensed version of this paper was presented orally (Warshaw and Smith, 1980). The agpaitic index (alkalis/alumina) and the other Al-saturation index

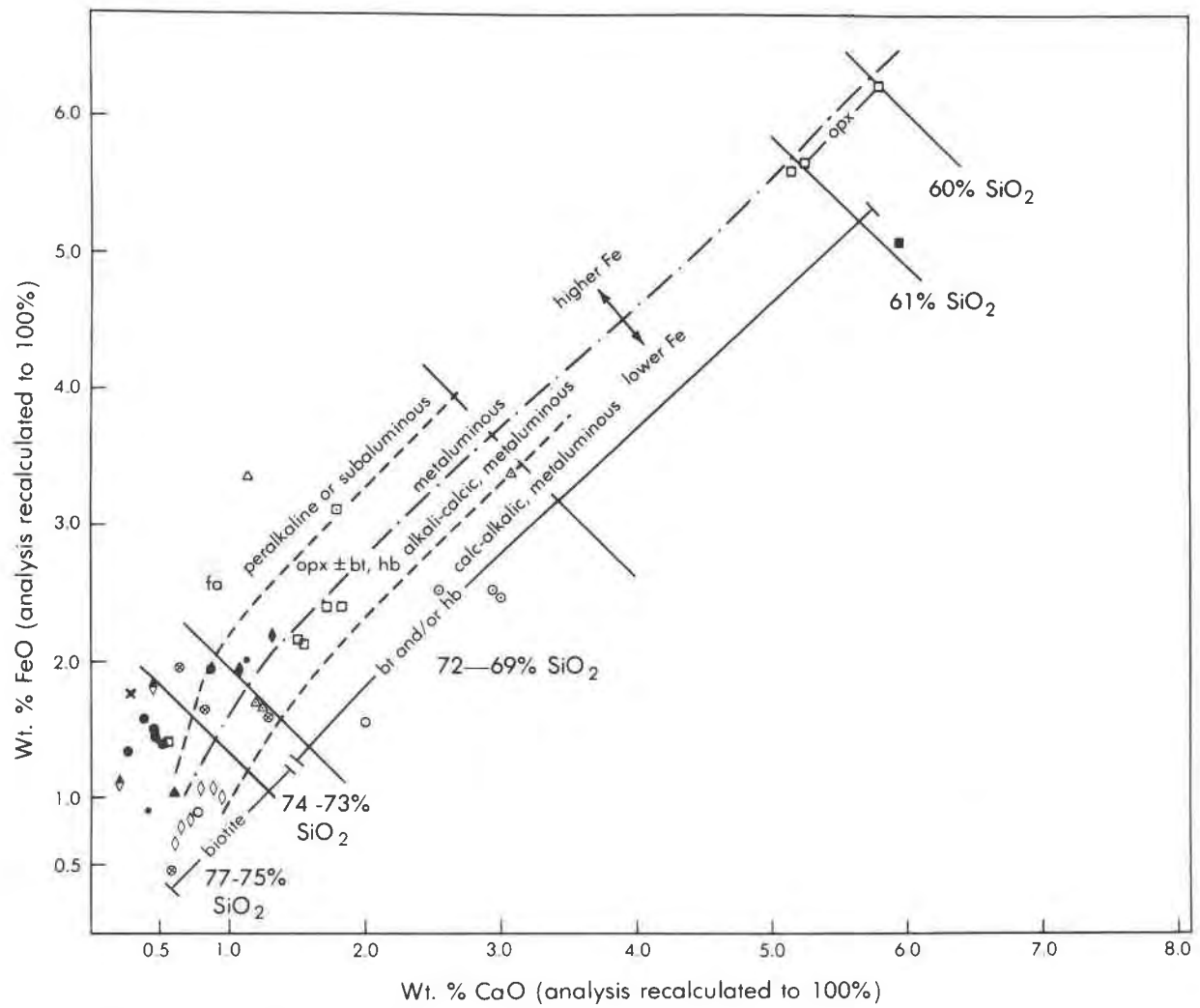

Fig. 4. Plot of total Fe as FeO vs. CaO in the whole rocks for all those salic volcanics of Fig. 3. The symbols and abbreviations are given in Table 6. The solid lines with negative slope separate areas of comparable silica percentages. The dashed lines separate the rocks according to phenocryst type and alumina saturation or CaO enrichment. The dot-dash line separates them into higher- and lower-Fe types.

indicate the degree of polymerization of the aluminosilicate portion of a silicate melt. When these indices are close to 1.00, the NBO/T is close to zero. It increases with decreasing Al-saturation indices, i.e., with greater amounts of Al than can be charge-balanced in tetrahedral coordination. Mysen et al. (1985) showed that the Fe^{3+}/Fe^{2+} ratio increases with increasing NBO/T (decreasing polymerization) and Al/(Al + Si). They also found that the increase in Fe^{3+}/Fe^{2+} ratio, a linear function of the Z/r^2 (ionization potential) of network-modifying cations in Al-free silicate systems, is enhanced in aluminous systems with increasing NBO/T. Such enhancement is indicated in Table 7, which includes both FeO/CaO ratios and Al-saturation indices.

All of the Bandelier Tuff rocks that contain fayalite phenocrysts (subunits I–III) have Al-saturation indices close to 1.0. The clinopyroxenes in these rocks contain no more than 0.30% Al_2O_3, all of it being tetrahedral. Subunit IV clinopyroxenes have 0.4% of this constituent. The clinopyroxene from the subunit V sample has more than enough Al (0.91% Al_2O_3) to fill the tetrahedral position in this metasilicate. The Al-saturation indices of this particular ash flow indicate that there is more Al in this rock than can be charge-balanced by alkalis and alkaline earths in an aluminosilicate network.

The compositions of the pyroxenes in the rhyolites are influenced by all the whole-rock ratios listed in Table 7 but not by the molar ratio of total Fe to Mg for those peralkaline or subaluminous rhyolites containing very little Mg. It is the ratio of Fe^{2+} to Mg in the magma that influences the location of the pyroxenes on the pyroxene quadrilateral. The difference between the total Fe/Mg and the pre-eruptive Fe^{2+}/Mg ratios was probably greater for the Bandelier Tuff than for the Sierra La Primavera

TABLE 7. Molar ratios and types of rocks and phenocrysts of salic volcanic rocks

Sample identification and/or locality*		Agpaitic index	$\frac{CaO + Na_2O + K_2O}{Al_2O_3}$	$\frac{FeO^{**}}{CaO}$	Phenocrysts†	Type	$\frac{FeO^{**}}{FeO^{**} + MgO}$
				Part A. >76% silica			
Sierra La Primavera		1.055	1.097	5.07	fa	slightly peralkaline	0.95
Lava Creek Tuff, early		0.916	0.951	3.58	fa	subaluminous	0.98
Bandelier Tuff							
Guaje Pumice Bed		0.969	1.007	3.93	fa	subaluminous	0.93
	B5	0.953	1.009	3.22	fa	subaluminous	0.92
	1	0.970	1.037	2.57	fa	subaluminous	0.94
	30	0.975	1.045	2.44	fa	subaluminous	0.88
	2	0.979	1.063	1.94	opx, fa	subaluminous	0.79
Mono Craters	6	0.946	1.035	1.31	fa	subaluminous	0.93
	5	0.950	1.036	1.36	fa	subaluminous	0.93
	19	0.941	1.028	1.33	opx	subaluminous	0.97
	16	0.942	1.031	1.29	opx	subaluminous	0.93
	17	0.943	1.029	1.34	opx	subaluminous	0.95
	15	0.941	1.028	1.32	opx	subaluminous	0.93
Bishop Tuff	104	0.902	0.998	0.94	bt	subaluminous	0.93
	88	0.911	0.997	0.89	opx, bt	subaluminous	0.97
	107	0.928	1.025	0.98	opx, bt	alkali-calcic	0.87
Long Canyon		0.853	0.934	0.61	bt	peraluminous	0.93
Topopah Spring, rhy		0.904	0.963	1.74	bt	metaluminous	0.63
Los Chocoyos, hi-K		0.875	0.997	0.73	bt	metaluminous	0.68
				Part B. >75% silica			
Lava Creek Tuff, late		0.882	0.948	2.93	fa	metaluminous	0.90
Bishop Tuff	72	0.901	1.016	1.00	opx bt	alkali-calcic	0.73
	78	0.874	1.001	0.91	opx bt	alkali-calcic	0.80
	77	0.910	1.050	0.81	opx bt	alkali-calcic	0.62
Los Chocoyos, low-K		0.729	0.991	0.61	amph	calc-alkalic	0.68
				Part C. 70–72% silica			
Oraefajokull		1.019	1.171	2.36	fa	peralkaline	0.97
Bandelier Tuff	6	0.853	0.961	1.74	opx	metaluminous	0.83
Inyo Craters	23	0.892	1.024	1.43	hb bt	metaluminous	0.80
	24	0.868	1.025	1.41	hb bt	metaluminous	0.75
Ceboruco	122	0.821	0.994	1.12	bt	metaluminous	0.76
	364	0.792	0.971	1.10	hb	metaluminous	0.76
Lassen	28	0.697	1.018	0.77	hb bt	calc-alkalic	0.57
	29	0.691	1.048	0.67	hb bt	calc-alkalic	0.53
	27	0.677	1.046	0.63	hb bt	calc-alkalic	0.49

Note: Data listed in each part in order of increasingly higher oxygen-buffer curves (Fig. 3). Each part is based on percentages of silica in Table 6.
* See Table 6 for references, complete sample designation, and abbreviations.
** Moles total Fe calculated as FeO.
† cpx is also present with fa and opx.

rhyolites (Mahood, 1980, 1981) and even greater for the Bishop Tuff (Hildreth, 1977, 1979).

CONCLUSIONS

The compositions of the ferromagnesian silicates in the Tshirege Member of the Bandelier Tuff and the corresponding pre-eruptive temperatures vary in a regular way with the stratigraphic sequence. The clinopyroxene and fayalite occurring in the basal air fall of this member of the Bandelier Tuff are the richest in Fe and Mn and poorest in Mg. The uppermost flow of this unit has the most Mg-rich pyroxenes and the highest pre-eruptive temperature. It came from the deepest, hottest zone of the magma chamber, the zone that had the highest Mg/Fe ratio according to Smith and Bailey (1966).

The change from fayalite to orthopyroxene during the eruption occurred when the material being erupted came from a zone that had been deep enough so that the Mg/Fe ratio was such that the low-Ca phase precipitating in equilibrium with the clinopyroxene contained enough Mg to stabilize Fe-bearing orthopyroxene at the pressure and temperature at that depth. The oxygen fugacity of the magma from the deeper zones in the chamber was determined to have been higher than that in the upper zones. The higher oxygen fugacity is compatible with the occurrence of orthopyroxenes rather than fayalites, which occur on or below the fayalite-magnetite-quartz buffer curve and have higher Fe^{2+}/Mg ratios than orthopyroxenes.

In a comparison of the properties of the Bandelier Tuff and its ferromagnesian silicate phenocrysts with other high-silica rhyolites containing little Mg, the following relationships are apparent. The location of the Bandelier and Lava Creek (Hildreth, 1981; Hildreth et al., 1984) tuffs between the fayalite-bearing Sierra La Primavera

rhyolites (Mahood, 1980) and the orthopyroxene-bearing Bishop Tuff (Hildreth, 1977) on both the oxygen fugacity–temperature plot and the pyroxene quadrilateral is related to the compositions and not to the temperatures of their magmas. Interrelationships were found among oxygen fugacity and certain aspects of magma composition. Thus, the Bandelier Tuff lies on higher oxygen-buffer curves than the Sierra La Primavera sample and has lower agpaitic indices and lower Fe^{2+}/Mg and Fe_{tot}/Ca ratios. The opposite is true in a comparison of most of the Bandelier Tuff with the Bishop Tuff. The Bandelier Tuff and all the volcanics plotted in the fayalite area of Figure 4 can be described as Fe-rich rhyolites. This includes the obsidians from Iceland as well as some of the high-silica rhyolites.

Acknowledgments

This study was made considerably easier by the help of the following colleagues at the U.S. Geological Survey: Nelson Hickling for collecting raw data on the manual electron microprobe, Lovell Wiggins for instruction in the use of the automated microprobe, and J. Stephen Huebner for discussions on the precision and accuracy of electron-microprobe analysis. Roy Bailey assisted R. L. Smith in the collection of some of the rock samples. The paper was improved as a result of the helpful reviews by Malcolm Ross and John C. Stormer, Jr. Donald H. Lindsley, State University of New York at Stony Brook, provided helpful advice concerning geothermometry and geobarometry. He supplied the data on temperature and oxygen fugacity obtained with the latest (1988) version of the silicate-oxide geothermometer on which he worked with B. R. Frost and D. J. Andersen. He also gave us computer programs for geothermometers.

References cited

Andersen, D.J., and Lindsley, D.H. (1988) Internally consistent solution models for Fe-Mg-Mn-Ti oxides: Fe-Ti oxides. American Mineralogist, 73, 714–723.

Bacon, C.R., and Duffield, W.A. (1981) Late Cenozoic rhyolites from the Kern Plateau, southern Sierra Nevada, California. American Journal of Science, 281, 1–34.

Bailey, R.A., Smith, R.L., and Ross, C.S. (1969) Stratigraphic nomenclature of volcanic rocks in the Jemez Mountains, New Mexico. U.S. Geological Survey Bulletin 1274-P, 1–19.

Bence, A.E., and Albee, A.L. (1968) Empirical correction factors for the electron microanalysis of silicates and oxides. Journal of Geology, 76, 382–403.

Buddington, A.F., and Lindsley, D.H. (1964) Iron-titanium oxide minerals and synthetic equivalents. Journal of Petrology, 5, 310–357.

Carmichael, I.S.E. (1967) The iron-titanium oxides of salic volcanic rocks and their associated ferromagnesian silicates. Contributions to Mineralogy and Petrology, 14, 36–64.

Douglas, E.W., Nath, P., and Paul, A. (1965) Oxygen ion activity and its influence on the redox equilibrium in glasses. Physics and Chemistry of Glasses, 6, 216–223.

Finger, L.W., and Hadidiacos, C.G. (1972) Electron microprobe automation. Carnegie Institution of Washington Year Book 71, 598–600.

Frost, B.R., Lindsley, D.H., and Andersen, D.J. (1988) Fe-Ti oxide-silicate equilibria: Assemblages with fayalitic olivine. American Mineralogist, 73, 727–740.

Hadidiacos, C.G., Finger, L.W., and Boyd, F.R. (1971) Computer reduction of electron-probe data. Carnegie Institution of Washington Year Book 69, 294.

Hewitt, D.A. (1978) A redetermination of the fayalite-magnetite-quartz equilibrium between 650 °C and 850 °C. American Journal of Science, 278, 715–724.

Hildreth, W. (1976) The Bishop Tuff: Compositional zonation in a silicic magma chamber without crystal settling. Geological Society of America Abstracts with Programs, 8, 918.

——— (1977) The magma chamber of the Bishop Tuff: Gradients in temperature, pressure and composition. Ph.D. thesis, University of California, Berkeley.

——— (1979) The Bishop Tuff: Evidence for the origin and compositional zonation in silicic magma chambers. In Chapin, C.E., and Elston, W.E., Eds., Ash-flow tuffs, Geological Society of America Special Paper 180, 43–75.

——— (1981) Gradients in silicic magma chambers: Implications for lithospheric magmatism. Journal of Geophysical Research, 86, 10153–10192.

Hildreth, W., Christiansen, R.L., and O'Neil, J.R. (1984) Catastrophic isotopic modification of rhyolitic magma at times of caldera subsidence, Yellowstone Plateau volcanic field. Journal of Geophysical Research, 89, 8339–8369.

Huebner, J.S., and Turnock, A.C. (1980) The melting relations at 1 bar of pyroxene composed largely of Ca-, Mg- and Fe-bearing components. American Mineralogist, 65, 225–271.

Izett, G.A. (1981) Recorders of upper Cenozoic silicic pyroclastic volcanism in the western United States. Journal of Geophysical Research, 86, 10200–10222.

Izett, G.A., and Wilcox, R.E. (1968) Perrierite, chevkinite and allanite in upper Cenozoic ash beds in the western United States. American Mineralogist, 53, 1558–1567.

Lindsley, D.H. (1983) Pyroxene thermometry. American Mineralogist, 68, 477–493.

Lindsley, D.H., and Andersen, D.J. (1983) A two-pyroxene thermometer. Proceedings, Thirteenth Lunar and Planetary Science Conference, Part 2. Journal of Geophysical Research, 88, Supplement, A887–A906.

Lipman, P. W. (1971) Iron-titanium oxide phenocrysts in compositionally zoned ash-flow sheets from southern Nevada. Journal of Geology, 79, 438–456.

Lipman, P.W., Christiansen, R.L., and O'Connor, J.T. (1966) A compositionally zoned ash-flow sheet in southern Nevada. U.S. Geological Survey Professional Paper 524-F.

Luhr, J.F., and Carmichael, I.S.E. (1980) The Colima volcanic complex, Mexico, I. Post-caldera andesites from Volcán Colima. Contributions to Mineralogy and Petrology. 71, 343–372.

Mahood, G.A. (1980) The geological and chemical evolution of a late Pleistocene rhyolitic center: The Sierra La Primavera, Jalisco, Mexico, Ph.D. thesis, University of California, Berkeley.

——— (1981) A summary of the geology and petrology of the Sierra La Primavera, Jalisco, Mexico. Journal of Geophysical Research, 86, 10137–10152.

Mahood, G.A., and Hildreth, W. (1983) Large partition coefficients for trace elements in high-silica rhyolites. Geochemica et Cosmochimica Acta, 47, 11–30.

Mysen, B.O., Virgo, D., and Seifert, F.A. (1979) Melt structures and redox equilibria in the system CaO-MgO-FeO-Fe_2O_3-SiO_2. Carnegie Institution of Washington Year Book 78, 519–526.

Mysen, B.O., Seifert, F.A., and Virgo, D. (1980) Structure and redox equilibria of iron-bearing silicate melts. American Mineralogist, 65, 867–884.

Mysen, B.O., Virgo, D., and Seifert, F.A. (1984) Redox equilibria of iron in alkaline earth silicate melts, relationships between melt structure, oxygen fugacity, temperature and properties of iron-bearing silicate liquids. American Mineralogist, 69, 834–847.

Mysen, B.O., Virgo, D., Neumann, E.R., and Seifert, F.A. (1985) Redox equilibria and structural states of ferric and ferrous iron in melts in the system CaO-MgO-Al_2O_3-SiO_2-Fe-O: Relationships between redox equilibria, melt structure and liquidus phase equilibria. American Mineralogist, 70, 317–331.

Nelson, S.A. (1979) The geology and petrology of Volcán Ceboruco, Nayarit, Mexico, and partial molar volumes of oxide components of silicate liquids. Ph.D. thesis, University of California, Berkeley.

Rose, W.I., Jr., Grant, N.K., and Easter, J. (1979) Geochemistry of the Los Chocoyos Ash, Quezaltenango Valley, Guatemala. In Chapin, C.E., and Elston, W.E., Eds., Ash-flow tuffs, Geological Society of America Special Paper 180, 87–99.

Seifert, F.A., Mysen, B.O., and Virgo, D. (1982) Three-dimensional network melt structure in the systems SiO_2-$NaAlO_2$, SiO_2-$CaAl_2O_4$, and SiO_2-$MgAl_2O_4$. American Mineralogist, 67, 696–719.

Shaw, H.R., Smith, R.L., and Hildreth, W. (1976) Thermogravitational mechanisms for chemical variations in zoned magma chambers. Geological Society of America Abstracts with Programs, 8, 1102.

Simmons, E.C., Lindsley, D.H., and Papike, J.J. (1974) Phase relations and crystallization sequence in a contact-metamorphosed rock from Gunflint Iron Formation, Minnesota. Journal of Petrology, 15, 539–565.

Smith, R.L. (1979) Ash-flow magmatism. In C.E. Chapin and W.E. Elston, Eds., Ash-flow tuffs, Geological Society of America Special Paper 180, 5–27.

Smith, R.L., and Bailey, R.A. (1966) The Bandelier Tuff: A study of ash-flow eruption cycles from zoned magma chambers. Bulletin of Volcanology, 29, 83–104.

Warshaw, C.M., and Smith, R.L. (1980) Ferromagnesian silicates in the Bandelier Tuff. Geological Society of America Abstracts with Programs, 12, 545.

Manuscript received July 24, 1984
Manuscript accepted April 25, 1988